Figure S1 Dnmt3b expression was reduced in fracture callus from diabetic and aging mice. Real-time qPCR analyses were performed to determine the relative expression of *Dnmt3b* in 7 dpf fracture callus from (A) high-fat diet fed (n=5) and (B) 18-month-old mice (n=5). Data was presented as means ± SD. * indicates $p < 0.05$ by Student's *t* test.

Figure S2 Dnmt3b ablation in MPCs showed no cortical and trabecular bone difference in adult mice. (A) Body weight of 10-weeks-old control and *Dnmt3b*^{Prx1} mice (n=10). 3D images of cortical bone (B) and metaphyseal trabecular bone (C) from 10-week-old control and *Dnmt3b*^{Prx1} mice (n=5). (D) Cortical thickness (Ct.Th), tissue mineral density (TMD), bone area and polar moment of inertia (pMOI), bone volume fraction (BV/TV), trabecular number (Tb.N), trabecular thickness (Tb.Th) and trabecular spacing (Tb.Sp) were calculated (n=5). Data was presented as means ± SD.

Figure S3 In vivo Dnmt3b deletion efficiency in MPCs during fracture repair. (A) Western blot analyses for Dnmt3b were conducted on protein lysates from femurs and tibia of *Dnmt3b*^{Prx1} mice and control mice at 10-weeks of age (n=3). (B) Immunohistochemical (IHC) staining for Dnmt3b was performed on fracture callus sections of *Dnmt3b*^{Prx1} and control mice at 7 dpf (n=5). Scale bar, 50μm.

Figure S4 Dnmt3b ablation did not affect MPCs proliferation in vitro. (A) CFU-F assays were performed on bone marrow-derived MPCs from 10-week-old *Dnmt3b*^{Prx1} and control mice (n=3). (B) Quantification of type I colonies (CFU-Fs) was performed on crystal violet staining (n=3). Data was presented as means ± SD.

Figure S5 Dnmt3b LOF led to DNA hypomethylation in Rbpjκ. Methyl-qPCR was performed on genomic DNA isolated from control and Dnmt3b LOF cells. Specific primers were used to

examine the methylation status of CpG island 1 and 2 respectively.

Figure S6 Notch inhibition via DAPT restored differentiation of *Dnmt3b*^{prx1} MPCs. (A) MPCs isolated from E11.5 limb buds of *Dnmt3b*^{Prx1} and control pups were treated with DAPT to suppress Notch pathway for 3 days. Alcian blue staining was performed on micromass cultures (n=3). (B) Alcian blue intensity was measured by Image J (n=3). (C) Real-time qPCR analyses were performed to determine the relative expression of *Dnmt3b*, *HeyL*, *Sox9*, *Col2a1 and Agc1* in the micromass cultures. The mRNA levels were normalized to that of *Actb* and then were normalized to the vehicle-treated control group (n=3). (D) Bone marrow derived MPCs from *Dnmt3b*^{Prx1} and control mice were also treated with DAPT for up to 14 days. ALP (Alkaline phosphatase) staining and Alizarin Red staining were performed to examine osteogenic differentiation and mineral deposition (n=3). (E) ALP and Alizarin Red intensity was measured by Image J (n=3). (F) Real-time qPCR analyses were performed to determine the relative expression of *Dnmt3b*, *HeyL*, *Runx2* and *Spp1* in marrow-derived MPCs. The mRNA levels were normalized to that of *Actb* and then were normalized to the vehicle-treated control group (n=3). Data was presented as means ± SD. * indicates $p < 0.05$ by two-way ANOVA test.

Figure S7 Notch inhibition via DAPT restored osteoclast function in vivo. (A) TRAP (Tartrate-resistant acid phosphatase) staining of fracture callus sections of DAPT and DMSO treated control and *Dnmt3b*^{Prx1} mice at 14 days post fracture (n=5). Scale bar, 200μm. (B) Histomorphometry analysis of Oc. S/BS (osteoclast surface per bone surface) was performed on TRAP staining of DAPT and DMSO treated control and *Dnmt3b*^{Prx1} mice at 14 days post fracture (n=5). Data was presented as means ± SD. * indicates $p < 0.05$ by two-way ANOVA test.

Fig. S1

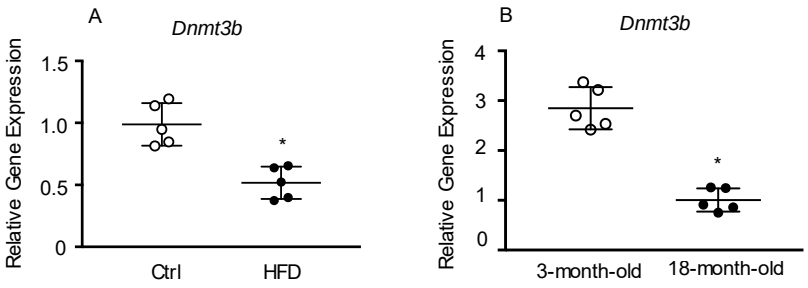
A
Dnmt3b
Relative Gene Expression
1.5
1.0
0.5
0
*
Ctrl
HFD
B
Dnmt3b
Relative Gene Expression
4
3
2
1
0
*
3-month-old
18-month-old

Fig. S2

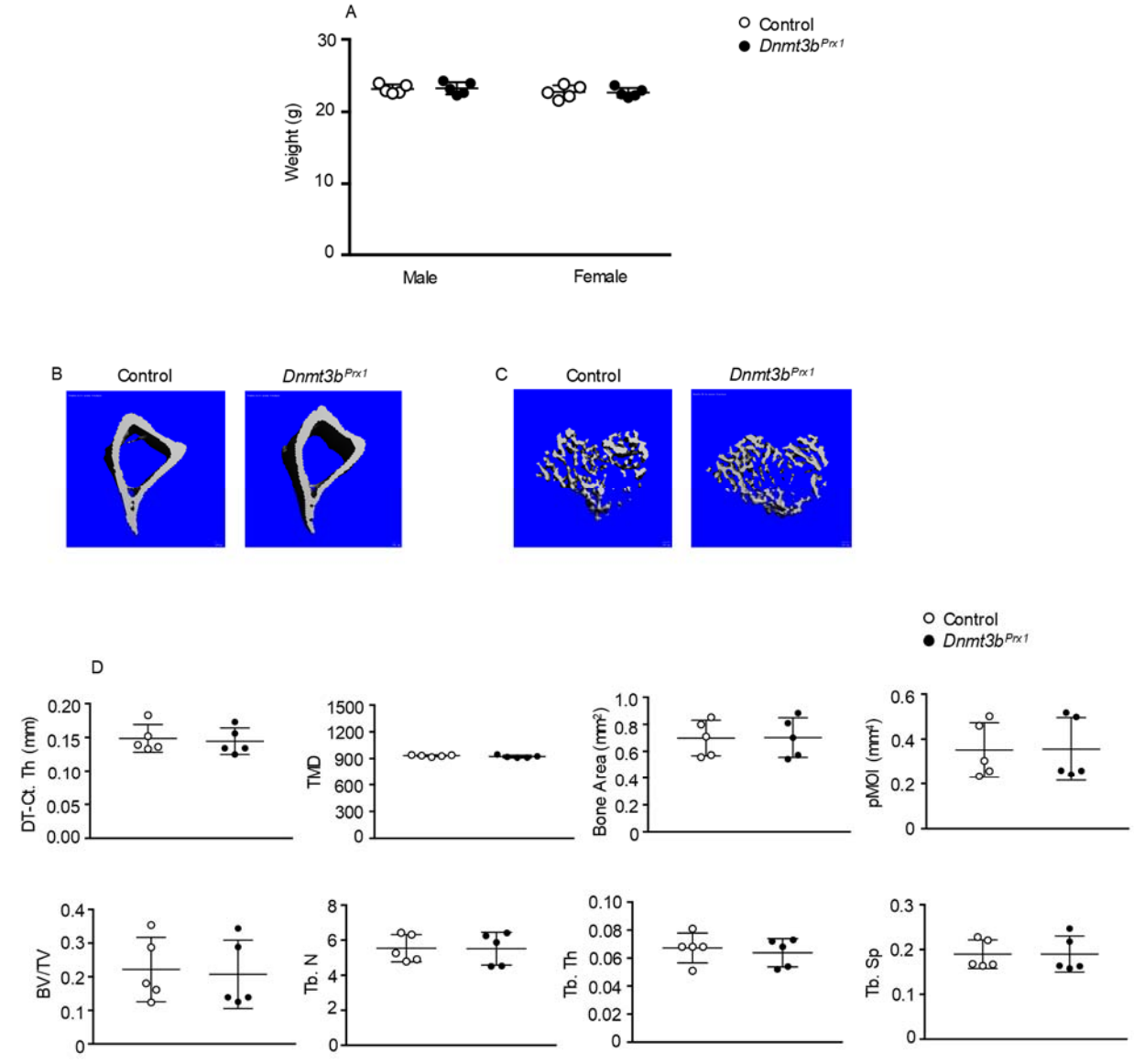
A
Control
Dnmt3b Prx1
Weight (g)
30
20
10
0
Male
Female
B
Control
Dnmt3b Prx1
C
Control
Dnmt3b Prx1
D
Control
Dnmt3b Prx1
DT-Ct. Th (mm)
TMD
Bone Area (mm²)
pMOI (mm⁴)
BV/TV
Tb. N
Tb. Th
Tb. Sp

Fig. S3

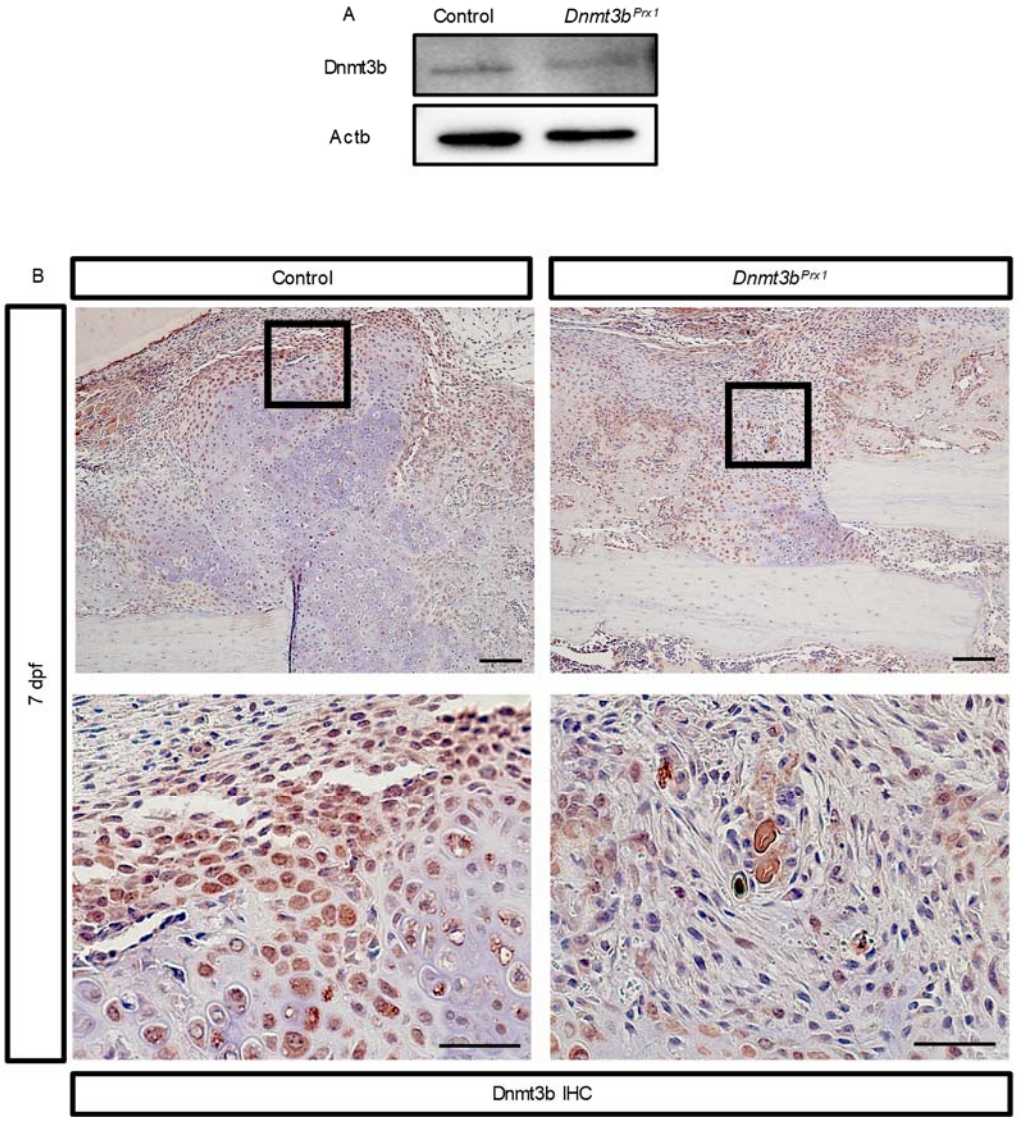
A
Control
Dnmt3b Prx1
Dnmt3b
Actb
B
Control
Dnmt3b Prx1
7 dpf
Dnmt3b IHC

Fig. S4

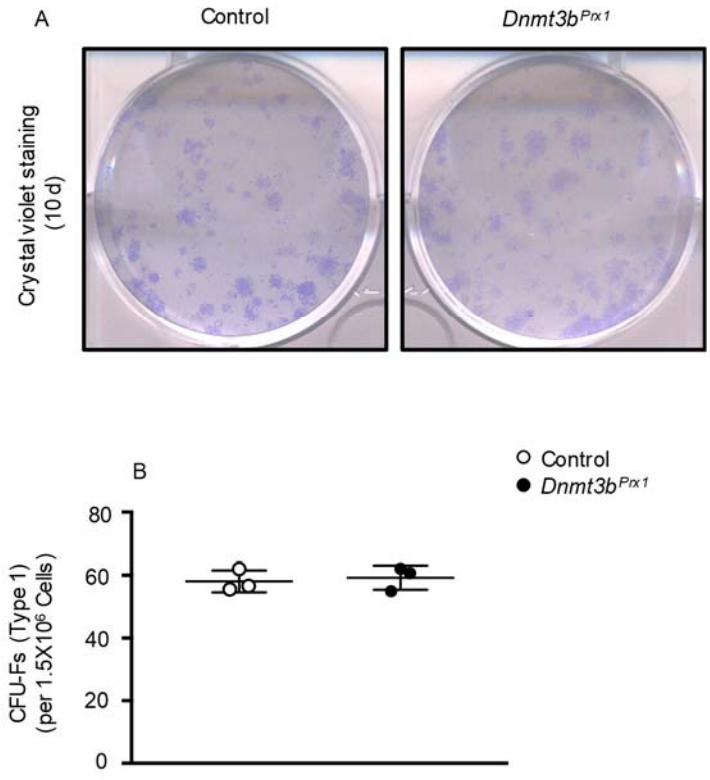
A
Control
Dnmt3b^Prx1
Crystal violet staining (10 d)
B
Control
Dnmt3b^Prx1
CFU-Fs (Type 1) (per 1.5X10^6 Cells)
80
60
40
20
0

Fig. S5

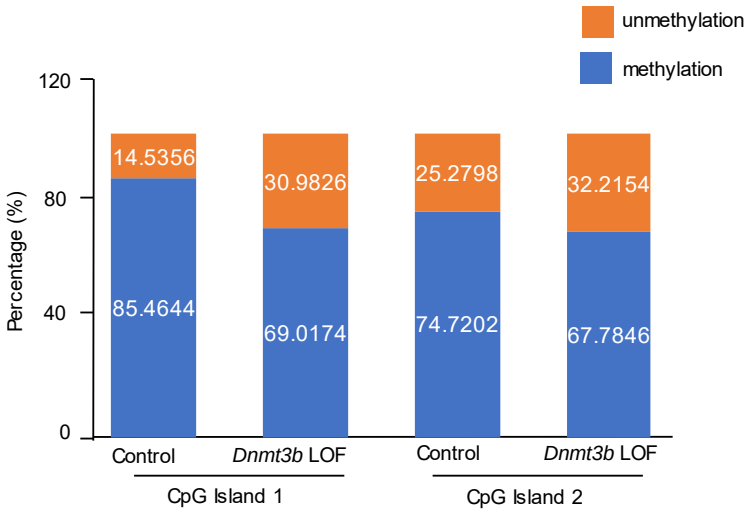
unmethylation
methylation
120
80
40
0
Percentage (%)
14.5356
85.4644
30.9826
69.0174
25.2798
74.7202
32.2154
67.7846
Control
Dnmt3b LOF
Control
Dnmt3b LOF
CpG Island 1
CpG Island 2

Fig. S6

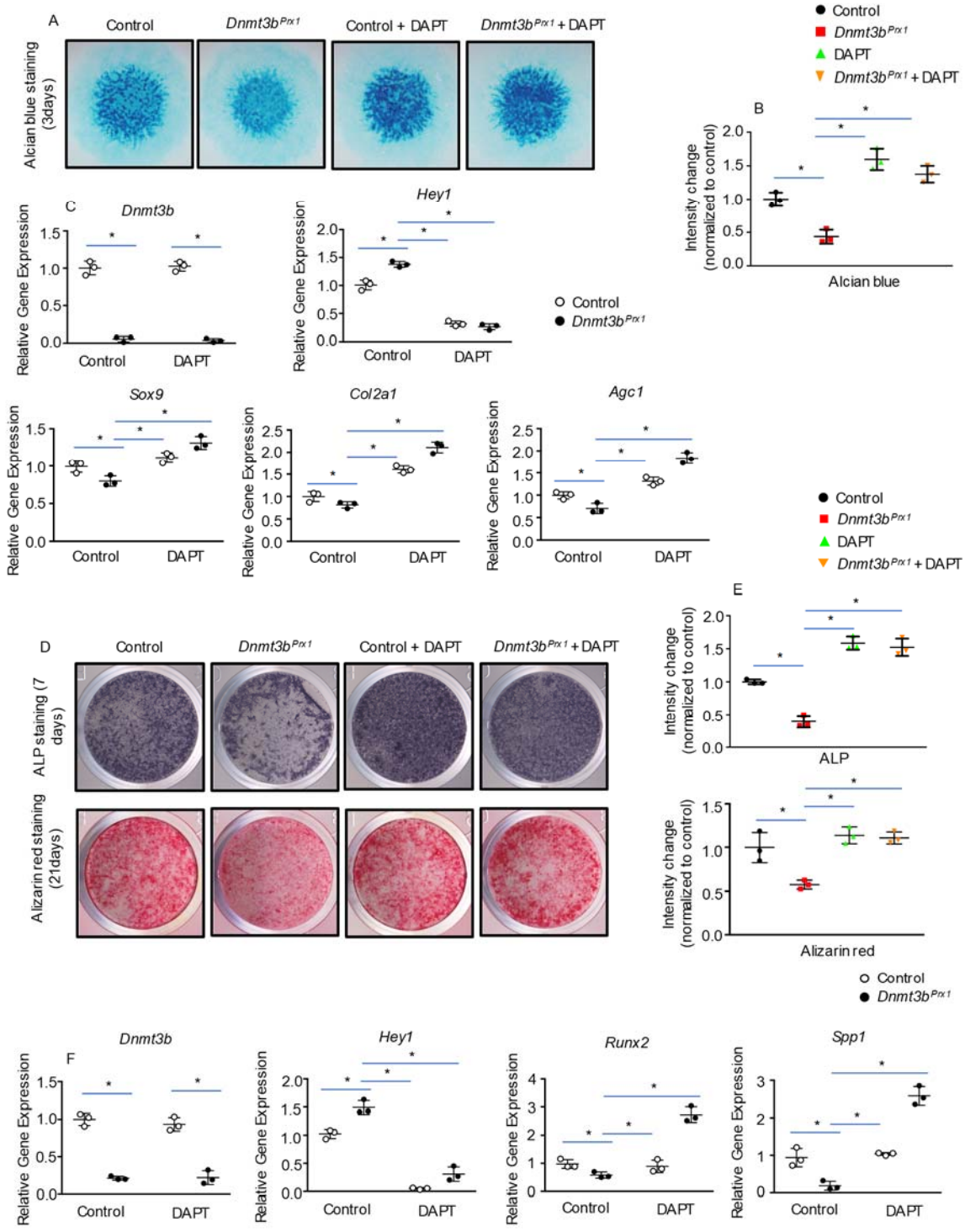
A
Control
Dnmt3b^Prx1
Control + DAPT
Dnmt3b^Prx1 + DAPT
Alcian blue staining (3days)
B
Control
Dnmt3b^Prx1
DAPT
Dnmt3b^Prx1 + DAPT
Intensity change (normalized to control)
Alcian blue
C
Dnmt3b
Hey1
Relative Gene Expression
Control
DAPT
Sox9
Col2a1
Agc1
D
ALP staining (7 days)
Alizarin red staining (21days)
E
ALP
Alizarin red
F
Runx2
Spp1

Fig. S7

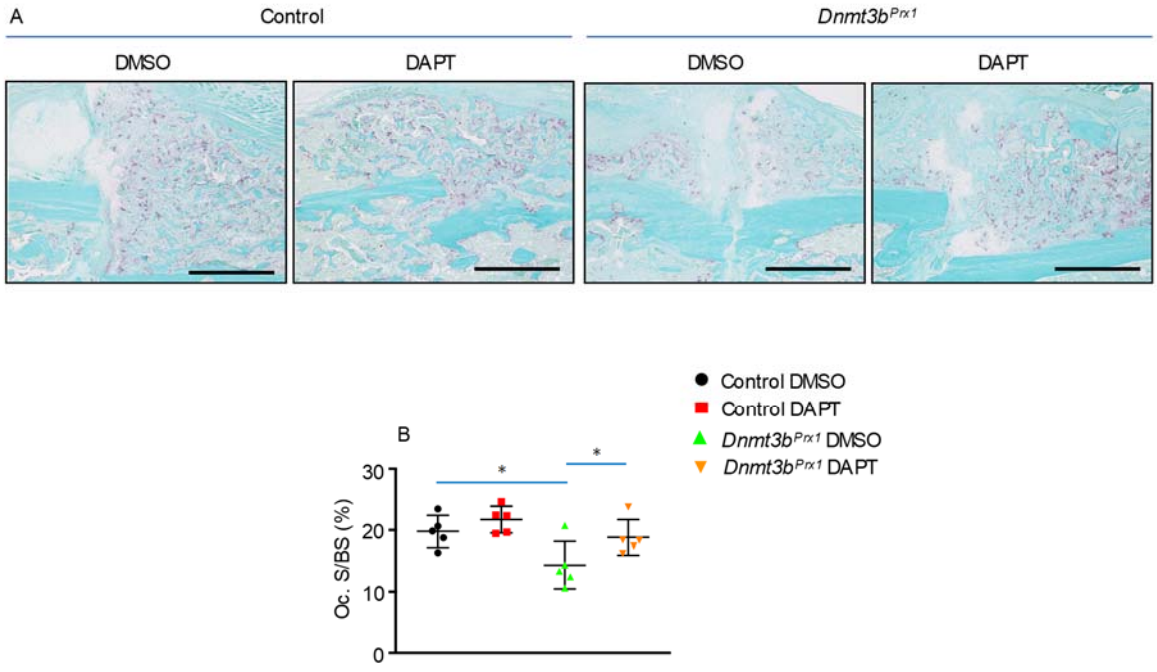
A
Control
Dnmt3b^Prx1
DMSO
DAPT
DMSO
DAPT
B
Control DMSO
Control DAPT
Dnmt3b^Prx1 DMSO
Dnmt3b^Prx1 DAPT
Oc. S/BS (%)
30
20
10
0
*
*